

Unveiling the mystery of nucleation and growth of carbon nanotubes in a pure carbon-arc

Soumen Karmakar*

*Department of Physics
Birla Institute of Technology, Mesra
Off-Campus Deoghar
Deoghar 814142, Jharkhand, INDIA*

**Email: skarmakar@bitmesra.ac.in; alternatively: Scorpioprince@gmail.com*

Since the discovery of carbon nanotubes (CNTs) in an electric-arc¹, this novel material has made a huge impact in the field of nanotechnology through a large number of potential applications². Though arc-plasma is known to be a source of pristine CNTs, the associated nucleation and growth processes are not understood well. In spite of numerous efforts³⁻⁸, the mystery still remains alive⁹ as none of the existing theories can satisfactorily explain why pure carbon-arc never produces single-walled CNTs (SWNTs). The answer is of fundamental importance not only for the sake of knowledge; it can even save thousands of existing patents from being expired¹⁰. Based on evidences hitherto overlooked and analysis of fracture mechanics, this letter highlights a mechanism that can decipher the mystery. It is shown that scrolled graphitic nanoribbon, which is certainly not a gas-phase condensate and has more than one layer, is the seed structure that can initiate CNT-growth in a pure carbon-arc. The nature of plastic deformation of polycrystalline graphite, subject to an appropriate hot thermal shock, is the prime factor responsible for the formation of such CNTs. It is also pin-pointed why the formation mechanisms of SWNT and multi-walled CNT are mechanistically different in an arc-plasma process.

Considering the high temperature of a carbon-arc (~4000°C), it is natural that carbon would take its most thermodynamically-stable state¹¹. However, theoretical calculations^{12, 13} do not provide a consensus on what should be the most stable form in such a condition. To investigate the matter experimentally, we analyzed the cathode-deposits (CDs), corresponding to various operating conditions, in a system reported elsewhere¹⁴, by replacing the conventional graphite anode by another one that was fabricated by sintering the outer grey-shell-material of CDs, collected from pure carbon-arcs. The operating conditions were the optimum ones¹⁴ for synthesizing CNTs

while using graphite-anode. However, with the new anode, which is vitreous in nature, hardly any trace of CNT within the corresponding CDs was found, well convincing us of the fact that only carbon-vapor is not sufficient to yield CNTs, contravening the theories based on gas-phase condensation³. In addition, noting that the feedstock graphite liquefies only at a pressure of ~100 bar¹⁵, much above the pressure inside carbon-arcs, models based on liquid-phase-growth^{4,8} appear quite unrealistic and misleading.

To have a proper answer to what exactly happens inside a pure carbon-arc, while synthesizing CNTs, the structural deformation of the anode during arcing and the consequences thereafter must be given due importance. In general, polycrystalline graphite, containing tiny crystallites oriented randomly and glued together by loosely packed amorphous carbon layers along the grain boundaries¹⁵, is used as anode for the synthesis of CNTs. Individual graphene in each crystallite is composed of numerous grains separated by boundaries, where defects, e.g. voids and vacancies tend to segregate^{15,16}. Upon exposing a graphite anode/arc interface to a high-temperature-arc suddenly (Fig. 1a), the surface-region undergoes catastrophic failure on account of elastic waves generated by hot thermal shock (HTS), provided equation (1) of Ref. 17 is satisfied. During the failure, multiple primary inter-granular cracks (Cr_0), which while gliding along the grain boundaries, cleave the adjacent grains into flakes setting up first generation microbranching instability within the system (Fig. 1d,e) following a similar mechanism, reported elsewhere¹⁷. The heat generated due to debonding, associated with a moving first generation crack-microbranch (Cr_1), cannot be released to its environment in case of HTS unlike a cold thermal shock. Such an energy transfer mechanism gives rise to second-generation microbranches (Cr_2), which glide along the quilt boundaries present in the graphene layers^{15,16}.

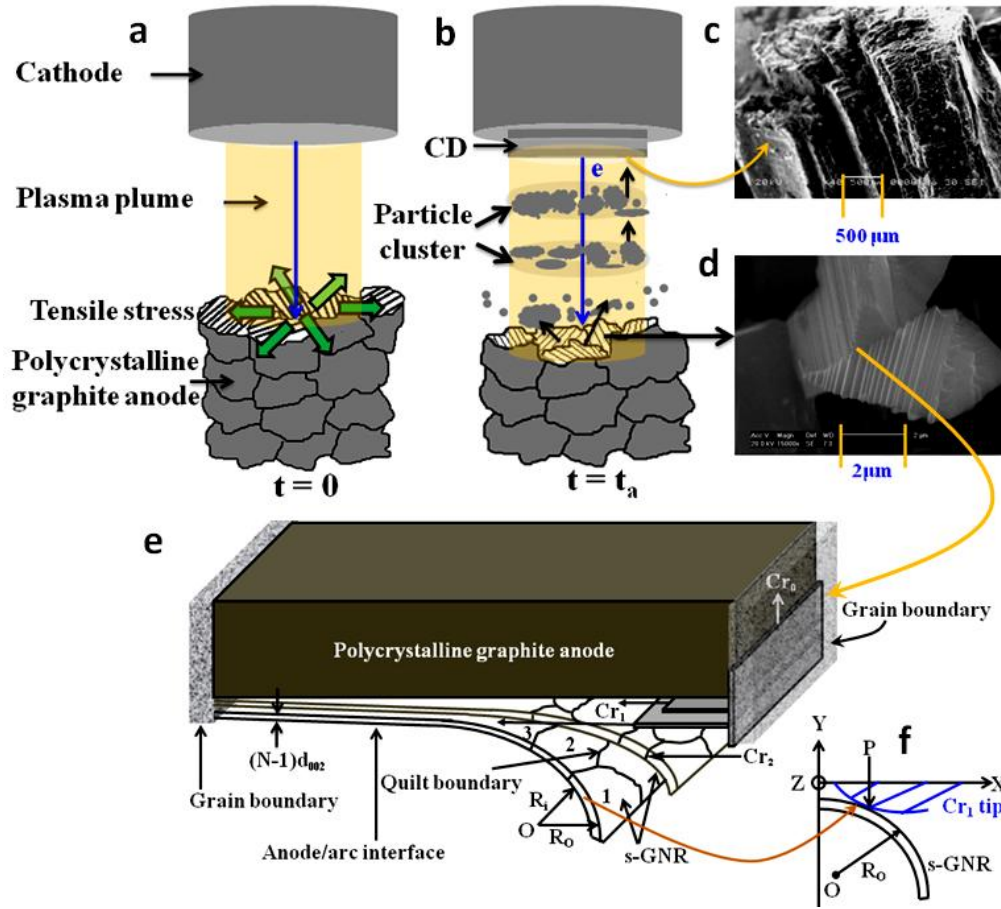


Figure 1 | Conceptual schematic of Dynamic fracture of graphite anode by HTS. **a**, The nature of stress experienced by an anode/arc interface upon exposure to an HTS at time $t=0$. **b**, Pulsed evaporation of anode as viewed at an arbitrary time t_a . **c**, SEM micrograph of vertical cross-section of a typical CD formed while synthesizing CNTs. Step like depositions in the CD is clearly visible. **d**, Typical fracture foot-prints present near the anode/plasma interface captured by an SEM after scraping off the shiny meniscus formed on the anode/arc interface after extinguishing a CNT-processing-arc slowly. **e**, Propagation of Cr_{1s} and Cr_{2s} through the anode-interior as a Cr_0 advances through a grain-boundary. s-GNRs, formed during this process enter the arc-zone in the sequence 1→2→3. **f**, Dependency of curvature of a s-GNR on the relative orientation and shape of the associated Cr_1 tip.

As the anode sublimates, a considerable fraction of the fed electrical energy converts into kinetic-energy of the sublimated mass, thereby decreasing the temperature of the freshly exposed anode/arc interface momentarily. Such a situation destroys the thermal equilibrium in between the arc and anode/arc interface thereby allowing another cycle of HTS to become operational. As a result of this, such carbon-arc generates spatially segmented particle clusters within the plasma zone, as shown in Fig.1b. Periodic fluctuations in the arc-voltage¹⁸ during evaporation of graphite-anode and Fig.1c are strong supporting evidences to validate the phenomenon.

During the instability, Cr_{1s} cleave the crystallites parallel to the (002) planes into rotationally misoriented graphitic flakes¹⁷ (r-GFs). The width of such r-GFs is given by $w = (N - 1)d_{002}$, with N and d_{002} being the number of layers present in the r-GFs and inter-planer separation of basal planes of graphite respectively, and depends on the thermo-elastic properties of the feedstock graphite, heat transfer

coefficient of the ambient and augmented temperature θ^{17} (which is a function of fed electrical power) of the arc-zone over the anode/arc interface. Here, a running Cr_0 is analogous to a mode-I crack expanding under uniaxial plane-stress in an infinite plate with $Lt \left(\frac{\text{length}}{\text{width}} \right) \rightarrow \infty$. Under such a condition, the corresponding stress intensity factor K_I reduces to $\sigma_T(\pi l)^{1/2}$, following the analysis by Rooke and Cartwright¹⁹; where σ_T and l are the applied thermal stress and the semi-crack-length respectively. Microbranching at a critical stress intensity factor K_{Ic} and crack-length l_c of Cr_0 is initiated inside the feedstock graphite when Cr_0 , after accelerating through a minimum distance l_c , releases its energy at a rate G_c per unit area to form 4 new Griffith surfaces parallel to the (002) planes on both sides of Cr_0 . Using the concepts of elastic continuum, Griffith's theory of brittle fracture²⁰ and the analysis by Irwin²¹, such a condition, in case of failure of polycrystalline graphite, leads to $G_c = 4\gamma = \frac{K_{Ic}^2}{E}$, with γ and E being the energy required to tear apart two adjacent (002) planes per unit

surface area created by Cr_1 and elastic modulus of polycrystalline graphite respectively. We therefore arrive at the following limiting condition, in which l_c represents the minimum value of w i.e. w_{min} .

$$K_{Ic} = \sigma_T(\pi w_{min})^{1/2} = 2(E\gamma)^{1/2} \quad (1).$$

Inserting the expression of σ_T in equation (1) and simplifying we get

$$w_{min} = \frac{4\gamma}{\pi\alpha^2\theta^2E} \quad (2),$$

where α is the coefficient of thermal expansion of polycrystalline graphite. In equation (2), all of γ , α , and E are functions of temperature. With the values of these parameters available in the literature¹⁵, we have a rough estimate that $w_{min} = \sim 10^{-10}m$ leading to $N_{min} > 1$ for $\theta = \sim 10^2 - 10^3 K$, the optimum range of θ to fracture the feedstock-graphite.

While Cr_1 s advance inside the crystallites, the associated r-GFs fragment mid-way into scrolled-graphitic-nanoribbons (s-GNRs) on account of Cr_2 s (Fig.1e). The radius of curvature (R_0) of the outer surface of such an s-GNR, depends on the dimension of the GNR, width of associated Cr_1 and curvature at the point of contact 'P' (Fig. 1f) of the crack-tip. During the failure, the evaporated amorphous content present in the vicinity of anode/arc interface escapes the anode in the form a vapor jet, which dislodges and drags the nascent s-GNRs formed on the anode/arc interface downstream (Fig.1e).

The s-GNRs, with $R_0=R_{min}$ (say), upon entering the plasma zone try to release their strain-energy by reducing their curvature, the probability of which reduces with the viscous drag and hence the mass-density of the ambient. If the vapor pressure near the anode approaches the solid-gas equilibrium saturated vapor pressure, s-GNRs retain their curvature; however with $R_0>R_{min}$. Otherwise, if $R_0>>R_{min}$ they flatten up to get back into the shape of GNR.

In case of a noisy arc, which is essential for graphite-sublimation²², there exists a temperature gradient on the anode/arc interface because of constriction of arc-root²² and anisotropic thermal transport property of graphite¹⁵. The situation changes the crack-dynamics at various locations of the anode thereby affecting the values of N and R_0 over a wide range.

Since the edge-state carbon atoms present in s-GNRs are highly reactive and unstable, they can bind easily with the most abundant C_3 species (~ 0.88 mole fraction), present near the anode²², to expand their surface area both laterally and longitudinally (Fig. 2) thereby minimizing their Gibb's free energy. This is chemically the most favorable reaction as such a transformation takes place at a non-equilibrium state and following the law of mass action, the reaction quotient Q corresponding to C_3 precursor is the highest among all the C_n species ($1 \leq n \leq 14$). Thus, the nucleation of a CNT is initiated by an s-GNR close to the anode at a high partial carbon-vapor-pressure and the process gets over once the growing edges of such an s-GNR, moving in the opposite directions along a circular arc, meet each other to form concentric seamless open cylinder (Fig.2). This structure is the proto CNT, (p-CNT) that can only grow along its axis as its open ends are the only sites, which contain unsaturated bonds (Fig. 2). Once nucleated, there is no change in the values of R_0 and N of a nascent p-CNT till it is fully grown by virtue of either diffusion or atomic readjustments, as these processes are intrinsically slow and negligible within the dwell-time ($\sim \mu s$) of the p-CNT within the arc.

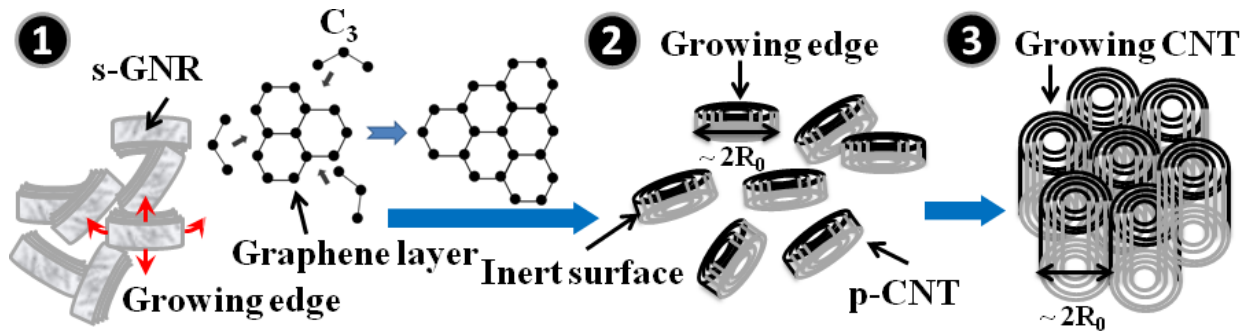


Figure 2| Nucleation and growth of CNT. The s-GNRs at step 1 converts into p-CNTs, as shown in step 2, by accommodating C_3 precursors in their graphene layers. p-CNTs then keep growing, as depicted in step 3, only along their axial directions reacting with the same precursor till the open ends are finally capped near the cathode surface, where they are finally disposed.

The radius of curvature R_o of the outer surface of such a nascent p-CNT is fairly a constant provided the standard deviations of the characteristic dimension of the GNRs and θ are appreciably low. In such a case, the inner radius of the tube R_i decreases with increase in N , exactly similar to what was highlighted by Iijima¹. As $N_{min} > 1$, a pure carbon-arc is incapable of producing SWNTs, hence confirming that the formation this specie has to be mechanistically different from that of MWNTs. On the other hand, a low partial carbon-vapor-pressure in the proximity of anode/plasma interface leads to formation of 2D layered structures, like few-layer-graphene²⁴.

At the normal operational plasma temperature (~0.5eV), conducive to CNT formation, the degree of ionization is low and the plasma is mostly dominated by the neutrals, a fact well evidenced from the huge amount of soot deposited on the reactor chamber walls during CNT synthesis¹⁴. The soot-forming-precursors, which deviate from the arc-electric-field lines, are indicative of a diffusion-dominated-process within the arc-zone.

As high partial vapor-pressure of carbon is essential for p-CNT growth, the arc-plasma, can therefore be considered as a solid/plasma colloid, where growing p-CNTs undergo Brownian motions. The corresponding motion and hence the time of flight of a growing p-CNT are similar to random walk amidst a large number of particles leading inevitably to collisions: the Brownian coagulation. As this two-phase colloid is thermodynamically unstable with respect to coarsening process, flocculation is provoked in such a system resulting in bundles of CNTs near the cathode region. The fact that arc-generated CNTs always appear in bundles, justifies the validity of the proposed mechanism.

All the C atoms on the growing-edge of a p-CNT are not identical in view of chemical reactivity because of the curvature induced strain²⁵. The atoms at the growing edge of the innermost shell hence are the most reactive and unstable, and their growth terminates faster than those residing outside at regions, which are deficient in C_3 precursors. Such terminations are common to all arc-generated CNTs¹⁸ and depend on the helicity of individual tube, along with relative spatial distribution of the terminal C atoms.

Arc-generated CNTs are always accompanied by a large number of particles with variable shapes and sizes. There are mainly two types of contributors in this connection. While the remnants of large graphitic chunks sputtered from the anode/arc interface during the sublimation process²² form the first group, the second one is formed by the particles nucleated within the arc as a result of gas-phase condensation.

The nucleated particles, which lack a well-defined crystalline structure and have low melting point on account of large surface to volume ratio, are finally condensed either on the CNTs or the electrode-surfaces following 'gas→liquid→solid' phase transitions at the completion of each HTS either in the form of slurry or shining thin film.

It is noteworthy that, similar to the conclusion by Gupta⁸, the presented model also does not recognize any effect of the cathode on the formation of CNTs, except recognizing it as a source of electrons to keep the arc alive.

Acknowledgements

The author is indebted his teachers S. V. Bhoraskar and A. K. Das, without whose kind blessings the proposed mechanism would possibly have never been conceptualized. Thanks are due to the Department of Physics, Savitribai Phule Pune University for permitting the author to record the SEM micrographs presented in the article.

1. Iijima, S. Helical microtubules of graphitic carbon. *Nature* **354**, 56-58 (1991).
2. Baughman, R. H., Zakhidov, A. A. & de Heer, W. A. Carbon nanotubes—the route toward applications. *Science* **297**, 787—792 (2002).
3. Gamaly, E. G. & Ebbesen, T. W. Mechanism of carbon nanotube formation in the arc discharge. *Phys. Rev. B* **52**, 2083—2089 (1995).
4. de Heer, W. A., Poncharal, P., Berger, C., Gezo, J., Song, Z., Bettini, J. & Ugarte., D. Liquid Carbon, Carbon-Glass Beads, and the Crystallization of Carbon Nanotubes *Science* **307**, 907—910 (2005).
5. Louchev, O. A., Sato, Y. & Kanda, H. Morphological stabilization, destabilization, and open-end closure during carbon nanotube growth mediated by surface diffusion. *Phys. Rev. E* **66**, 011601-1—011601-17 (2002).
6. Liu, Y. W., Wang, L. & Zhang, H. A possible mechanism of uncatalyzed growth of carbon nanotubes. *Chem. Phys. Lett.* **427**, 142—146 (2006).
7. Harris, P. J. F., Tsang, S. C., Claridge, J. B. & Green M. L. H. High-resolution electron microscopy studies of a microporous carbon produced by arc-evaporation. *J. Chem. Soc. Faraday Trans.* **90**, 2799—2802 (1994).
8. Gupta, V. Graphene as intermediate phase in fullerene and carbon nanotube growth: A Young–Laplace surface-tension model. *Appl. Phys. Lett.* **97**, 181910-1—181910-3 (2010).
9. Das, R., Shahnavaz, Z., Ali, Md. E. & Hamid, S. B. A. Can we optimize arc discharge and laser ablation for well controlled carbon nanotube synthesis? *Nano. Res. Lett.* **11**, 1—23 (2016).
10. MacKenzie, K. J. See, C. W., Dunens, O. M. & Harris, A. T. Do single-walled carbon nanotubes occur naturally? *Nature nanotechnol.* **3**, 310 (2008).
11. Smalley, R. E. From dopyballs to nanowires. *Mater. Sci. Eng. B* **19**, 1—7 (1993).

12. Robertson, D. H., Brenner, D. W. & Mintmire, J. W. Energetics of nanoscale graphitic tubules. *Phys. Rev. B* **45**, 12592—12595 (1992).
13. Sawada, S. & Hamada, N. Energetics of carbon nanotubes. *Solid State Comm.* **83**, 917—919 (1992).
14. Karmakar, S., Kulkarni, N. V., Sathe, V. G., Srivastava, A. K., Shinde, M. D., Bhoraskar, S. V. & Das, A. K. A new approach towards improving the quality and yield of arc-generated carbon nanotubes. *J. Phys. D: Appl. Phys.* **40**, 4829—4835 (2007).
15. Pierson, H. O. *Handbook of carbon, diamond and fullerenes*. Park Ridge NJ: Noyes; p. 50—107, (1993).
16. Huang, P. Y., Ruiz-Vargas, C. S., van der Zande, A. M., Whitney, W. S., Levendorf, M. P., Kevek, J. W., Garg, S., Alden, J. S., Hustedt, C. J., Zhu, Y., Park, J., McEuen, P. L. & Muller, D. A. Grains and grain boundaries in single-layer graphene atomic patchwork quilts. *Nature* **469**, 389—392 (2011).
17. Karmakar, S., Nawale, A. B., Kanhe, S. H., Sathe, V. G., Mathe, V. L. & Bhoraskar, S. V. Tailored conversion of synthetic graphite into rotationally misoriented few-layer graphene by cold thermal shock driven controlled failure. *Carbon* **67**, 534-545 (2013).
18. Iijima, S. Growth of carbon nanotubes. *Mat. Sci. Engg. B* **19**, 172—180 (1993).
19. Rooke, D. P. & Cartwright, D. J. *Compendium of stress intensity factors*. Ministry of Defence. Procurement Executive. London: H. M. S. O (1976).
20. Griffith, A. A. The phenomena of rupture and flow in solids. *Phil Trans R Soc Lond A* **221**, 163—198 (1921).
21. Irwin, G. R. Analysis of stresses and strains near the end of a crack traversing a plate. *J. Appl. Mech.* **24**, 361—364 (1957).
22. Abrahamson, J. Graphite sublimation temperatures, carbon arcs and crystallite erosion. *Carbon* **12**, 111—141 (1974).
23. Palmer, H. B. & Shelef, M. Physics and chemistry of carbon, (Walker, P. L. Jr., ed.) vol. 4, Marcel Dekker, New York (1968).
24. Karmakar, S., Kulkarni, N. V., Nawale, A. B., Lalla, N. P., Mishra, R., Sathe, V. G., Bhoraskar, S. V. & Das, A. K. A novel approach towards selective bulk synthesis of few-layer graphenes in an electric arc. *J. Phys. D: Appl. Phys.* **42**, 115201 (1—14) (2009).
25. Dumitrică, T., Landis, C. M. & Yakobson, B. I. Curvature-induced polarization in carbon nanoshells. *Chem. Phys. Lett.* **360**, 182—188 (2002).